JOURNAL OF MODERN OPTICS, 1992, VOL. 39, NO. 2, 233–242

Linear trap for high-accuracy spectroscopy of stored ions†

M. G. RAIZEN‡, J. M. GILLIGAN,
J. C. BERGQUIST, W. M. ITANO and
D. J. WINELAND

Time and Frequency Division, National Institute of Standards and Technology, Boulder, Colorado 80303, USA

(*Received 3 July 1991; revision received 23 September 1991*)

Abstract. In a linear r.f. Paul trap, 'crystallized' structures of laser-cooled $^{199}Hg^{+}$ ions are observed. The ground-state hyperfine transition at 40·5 GHz is observed in microwave–optical double-resonance spectroscopy. Future prospects are also discussed.

1. Introduction

Trapping and cooling of large numbers of ions, each confined to much less than a wavelength of an atomic transition (the Lamb–Dicke regime), is of great interest for high-accuracy spectroscopy, improved frequency standards, and atom–radiation field experiments. In a quadrupole r.f. Paul trap, the kinetic energy of a single trapped ion is on the order of the secular energy, and confinment of a single ion to the Lamb–Dicke regime for an optical transition has been successfully demonstrated [1, 2]. For a single $^{199}Hg^{+}$ ion laser-cooled to the Doppler limit [3], the fractional second-order Doppler shift is $\langle \Delta\nu_{D2}/\nu_0 \rangle = -2{\cdot}3 \times 10^{-18}$ [4]. However, two or more ions in the trap are pushed by their mutual Coulomb repulsion from the centre of the trap, which leads to relatively large micromotion associated with the non-zero r.f. field and limits laser cooling and the achievable confinement [5–7].

The linear trap design is descended from a race-track-configuration r.f. trap, first used by Drees and Paul for short-term confinement of an electron-ion plasma [8] and later by Church for longer confinement of atomic ions [9]. Race-track traps consist of quadrupole r.f. electrodes, similar to those used in mass filters, bent to form a closed path. Charged particles feel a force toward the axis of the quadrupole and follow trajectories that carry them around the path formed by the trap electrodes. Dehmelt first suggested using a string of ions in a linear trap to suppress the second-order Doppler shift [10]. In race-track traps, the ions are usually free to move along the axis of the trap, but to satisfy the Lamb–Dicke criterion it is necessary to fix the position of each ion in this direction as well as in the radial direction. The linear trap described here uses a static electric field to confine the ions in the axial direction. Using a static field allows us to fix the axial positions of the ions, but sacrifices the race-track trap's ability to confine both positive and negative charges simultaneously. The static field also weakens the radial confinement, as will be discussed below.

‡ Present address: Department of Physics, University of Texas at Austin, Austin, Texas 78712, U.S.A.

0950-0340/92 $3·00

Prestage *et al.* [11] have trapped a cloud of $^{199}Hg^+$ ions elongated along the axis of a linear trap and have demonstrated a $^{199}Hg^+$ frequency standard with excellent frequency stability. Crystallized strings of laser-cooled $^{24}Mg^+$ ions have been observed in a race-track trap at the Max Planck Institute for Quantum Optics [12]. In our group at the National Institute of Standards and Technology (NIST), we have constructed a linear r.f. trap and have observed simple 'crystallized' linear structures of up to tens of $^{199}Hg^+$ ions [13]. By varying the axial well depth, we have also observed more complex structures.

In the next section we describe the principle of the linear trap and present the results of numerical simulations of ion configurations. We then describe our trap and present images of trapped 'crystallized' structures of ions. We next present preliminary observations of the 40·5 GHz ground-state hyperfine transition of $^{199}Hg^+$ using microwave–optical double-resonance spectroscopy with a trapped string of ions and discuss the potential for a microwave frequency standard. We conclude with a discussion of future experiments and prospects.

2. Linear trap, theory

Consider the trap shown in figure 1. The r.f. electric fields are transverse to the trap axis for the entire axial extent of the centre segment of the trap. We assume that near the trap axis the time varying potential is

$$\phi = \frac{V_0(x^2 - y^2)}{2R^2} \cos \Omega t, \tag{1}$$

where R is approximately equal to the distance from the axis to the surface of the trap electrodes. For sufficiently high drive frequency Ω this results in a harmonic pseudopotential well in the radial direction of the form

$$\phi_p = \frac{qV_0^2}{4m\Omega^2 R^4}(x^2 + y^2) = \frac{m}{2q}\omega_r^2(x^2 + y^2), \tag{2}$$

where $\omega_r \equiv qV_0/(\sqrt{2}m\Omega R^2)$ is the oscillation frequency in the radial direction. The confinement in the radial direction is identical to that of a quadrupole mass analyser [14].

To provide confinement along the axis of the trap, a static voltage U_0 is applied to the end sections. Determining the potential in the trap due to this static potential on

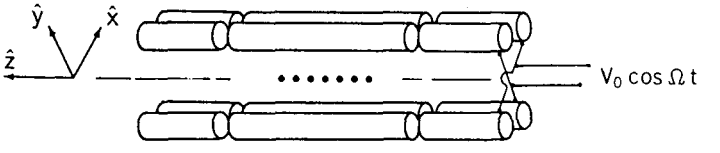

Figure 1. Linear trap configuration. An alternating r.f. voltage $V_0 \cos \Omega t$ is applied to diagonally opposite electrodes as shown. The segments of each rod are capacitively coupled so that each one can be biased at a different static potential, yet remain at the same r.f. potential. We assume that the end segments of the electrodes are long enough so that in the centre section of the trap the r.f. electric fields are parallel to the xy plane. To trap ions along z we assume the centre four electrodes are at static ground potential and the two sets of four electrodes on either end are at a static potential U_0 ($U_0 > 0$ to trap positive ions).

the electrodes would require a full three-dimensional calculation, which is beyond the scope of the present work. However, near the centre of the trap, the static potential can be approximated by

$$\phi_s = kU_0[z^2 - (x^2+y^2)/2] = \frac{m}{2q}\omega_z^2[z^2 - (x^2+y^2)/2], \tag{3}$$

where $\omega_z \equiv (2kqU_0/m)^{1/2}$ is the axial oscillation frequency in the trap and k is a geometric factor. The potential well in the radial direction is weakened by the addition of the static potential, and is given by

$$\phi_r = \frac{m}{2q}(\omega_r^2 - \omega_z^2/2)(x^2+y^2) = \frac{m}{2q}(\omega_r')^2(x^2+y^2), \tag{4}$$

where ω_r' is the radial oscillation frequency in the presence of the static potential and pseudopotential.

The kinetic energy in the micromotion of a string of ions trapped along the z axis can be about equal to the kinetic energy in the secular motion. At the Doppler cooling limit, the fractional second order Doppler shift can then be as low as $-2{\cdot}3 \times 10^{-18}$ for *all* the Hg^+ ions in the string [4]. We have performed numerical simulations to find ion configurations in a linear trap as a function of the number of ions and the radial and axial secular frequencies [15]. This calculation found the equilibrium positions of the ions by minimizing the potential energy, assuming harmonic potentials in the radial and axial directions and Coulomb repulsion between the ions.

The simplest configuration of ions is a linear string, which is obtained when the radial well is much deeper than the axial well. A computer simulation of eight ions in a string is shown in figure 2. The ions can be pushed into planar or three-dimensional configurations by increasing the axial well depth relative to that of the radial well. In figure 3 a planar zig–zag structure of 11 ions is shown. Such configurations are closely related to structures predicted for cold ions in storage rings [16].

3. Linear trap, experiment

The linear trap constructed in our group at NIST follows a geometry similar to the outline of figure 1. This design ensures that the r.f. fields are transverse to the trap axis. The trap dimensions are: rod diameters 1·6 mm, distance of the rod centres from the z axis of the trap 1·55 mm, and the axial centre trapping section 2·5 mm. The

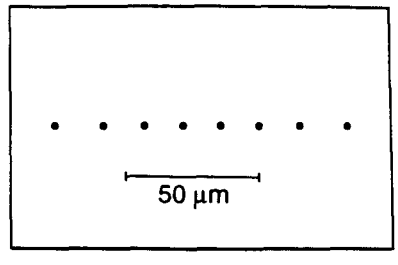

Figure 2. Numerical simulation of a crystallized string of eight $^{199}Hg^+$ ions for secular frequencies $\omega_r'/2\pi = 435$ kHz, $\omega_z/2\pi = 41{\cdot}7$ kHz. These secular frequencies were obtained by scaling secular frequencies measured under different conditions to the potentials applied to the trap when figure 5 was acquired.

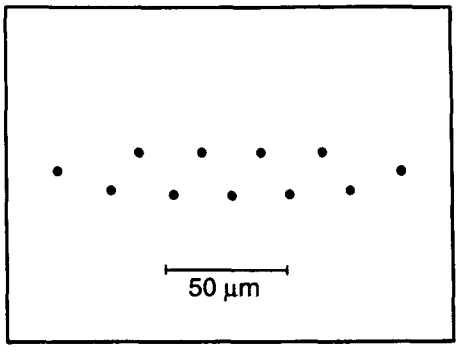

Figure 3. Numerical simulation of a crystallized zig–zag structure of 11 $^{199}Hg^{+}$ ions. An asymmetry in the two radial directions (x, y) was assumed, pinning the structure in the weaker of the two wells, and the projection is at 45° from the plane of the structure. The secular frequencies are $\omega_x'/2\pi = 77$ kHz, $\omega_y'/2\pi = 92{\cdot}4$ kHz, and $\omega_z/2\pi = 31$ kHz. These secular frequencies were obtained by scaling measured frequencies to the potentials applied when figure 6 was acquired and increasing ω_y' by 20% *ad hoc* to make the results agree with figure 6.

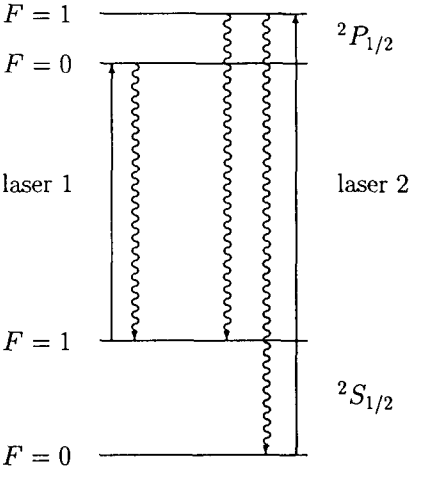

Figure 4. Energy level structure for the $^2S_{1/2}$ and $^2P_{1/2}$ levels of $^{199}Hg^{+}$ near zero magnetic field. The $^2S_{1/2}(F=0)-(F=1)$ hyperfine splitting is 40·5 GHz, and the $^2P_{1/2}(F=0)-(F=1)$ hyperfine splitting is 6·9 GHz. The intervals are not drawn to scale. Lasers 1 and 2 are used for cooling, optical pumping, and detection as described in the text.

radial size of the trap was chosen to permit Hg^{+} ions to be confined near the Lamb–Dicke regime for an optical transition by a 12·7 MHz r.f. drive with a voltage amplitude V_0 of approximately 700 V. In the work so far, amplitudes V_0 of up to 350 V were used. Axial confinement is achieved with a static voltage of typically 1 V or less. $^{199}Hg^{+}$ ions are loaded into the trap by leaking neutral ^{199}Hg (isotopic purity 91%) into the vacuum chamber to a pressure of approximately 10^{-6} Pa and then ionizing some of these atoms in the trap with electrons from a field emission point. After the trap is loaded, the chamber is evacuated to a pressure of approximately 10^{-8} Pa. The ions are laser-cooled by a few microwatts of c.w. laser radiation at 194 nm [2].

Due to the hyperfine structure of $^{199}Hg^+$, optical pumping must be considered in the laser cooling scheme. In figure 4 we show the hyperfine levels for the $^2S_{1/2}$ and $^2P_{1/2}$ states of $^{199}Hg^+$ in zero magnetic field. Two lasers at 194 nm are required. The ions are both cooled and detected using a laser (laser 1 in figure 4) that is tuned slightly below the resonant frequency of the optical transition $^2S_{1/2}(F=1) \rightarrow {}^2P_{1/2}(F=0)$. This is a 'cycling transition' since the ions that are excited to the $^2P_{1/2}(F=0)$ level can decay only to the $^2S_{1/2}(F=1)$ level according to dipole selection rules. The ions are detected by collecting photons scattered in this transition. Laser 1 can also weakly excite the $^2S_{1/2}(F=1) \rightarrow {}^2P_{1/2}(F=1)$ optical transition (it is detuned 6·9 GHz from this resonance, whose natural linewidth is $\gamma/2\pi = 70$ MHz). From the $^2P_{1/2}(F=1)$ level the ions can then decay to the $^2S_{1/2}(F=0)$ level. By itself, laser 1 would optically pump the ions into the $^2S_{1/2}(F=0)$ level, which would spoil the laser cooling. To prevent this, we have a second laser (laser 2 in figure 4), that is offset 47·4 GHz to the blue of laser 1 in order to repump the ions from the $^2S_{1/2}(F=0)$ level back to the $^2S_{1/2}(F=1)$ level. In addition to the above considerations, we must prevent optical pumping into the $^2S_{1/2}(F=1, m_F=\pm 1)$ levels. We do this by applying a magnetic field of about 5×10^{-4} T (5 G) at approximately 45° to the electric field vector of the 194 nm radiation.

To cool both the radial and axial motion of the ions, we direct the laser beam through the trap at an angle of approximately 9° to the trap axis. Fluorescence emitted perpendicular to the axis of the trap is collected by a fast lens system, which images it with a magnification of 22 onto an imaging photon detector. The secular frequencies of the trap are measured by applying a drive to the trap electrodes and observing a drop in the fluorescence (due to strong excitation of the secular motion of the ions) as the drive sweeps through resonance [17]. These measurements permit a quantitative comparison between the observed ion configurations and the numerical simulations described earlier. The secular frequencies were measured for several different r.f. and static voltages and had the correct functional dependence on the voltages. The unperturbed radial secular frequency ω_r was proportional to the r.f. voltage and the axial secular frequency ω_z was proportional to the square root of the static voltage. For very small axial voltage (less than 100 mV) the effects of local contact potentials can come into play, making it difficult to characterize the axial well depth. By changing the loading conditions (that is, by changing the neutral Hg background pressure and the duration and intensity of the field emission), we can trap different numbers of $^{199}Hg^+$ ions and have resolved as many as 33 ions in a string and as few as a single ion. To crystallize and resolve significantly longer strings, higher laser power and improved imaging optics will probably be required. Another limitation may be our ability to cancel the effects of local patch potentials over the entire axial extent of the string. In the present trap, static offsets can be independently applied to three of the four trapping rods to compensate for such potentials, but as the string of ions approaches the radial size of the trap (750 μm), these potentials may vary over the length of the string. In this case, we expect the static compensation to be less effective. In addition, we can apply a different static voltage to each end to translate the entire structure along the axis.

Two representative pictures of crystallized structures are shown in figures 5 and 6. In figure 5, eight ions in a string are clearly resolved. Figure 6 shows a structure of 11 ions (10 $^{199}Hg^+$ ions and one impurity ion). This structure was obtained by lowering the r.f. voltage on the trap for a fixed static voltage. Both ion configurations are in close agreement with the numerical simulations shown in figure 2 and in figure

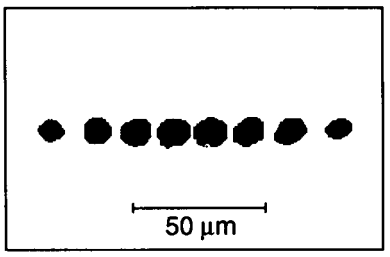

Figure 5. Image of crystallized string of eight $^{199}Hg^{+}$ ions. The potentials applied to the trap when this image was acquired were used as input for the numerical simulation shown in figure 2.

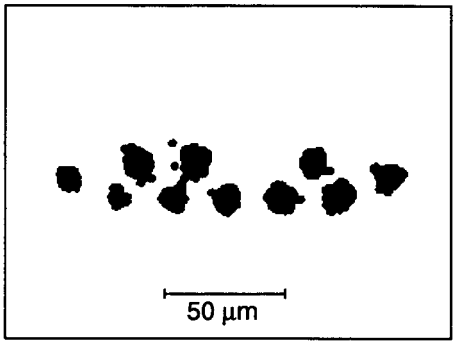

Figure 6. Image of a crystallized structure of ten $^{199}Hg^{+}$ ions and one impurity ion. The potentials applied to the trap when this image was acquired were used as input for the numerical simulation shown in figure 3.

3, which used secular frequencies that corresponded to the trap conditions for figures 5 and 6, respectively. These values were obtained by scaling secular frequencies measured under different trap conditions to the potentials applied to the trap when figures 5 and 6 were acquired. In order for the numerical simulation shown in figure 3 to agree with the ion configuration of figure 6 it was necessary to assume an azimuthal asymmetry in the radial potential sufficient to force the ions into a plane. The source of this asymmetry is not known, but it may be due to differences in contact potentials or static electric charges on the electrodes. For a large number of ions and a weak axial well, more complicated two and three-dimensional structures are seen. Such structures are closely related to the structures predicted for cold ions in storage rings [16]. A systematic and quantitative study of these two and three-dimensional crystallized structures will require eliminating the azimuthal asymmetry or characterizing it more completely.

4. Microwave–optical double-resonance

A string of cold ions is of great interest for high-resolution spectroscopy and improved frequency standards. With imaging techniques, each ion can be treated as an independent atomic clock, which is detected with 100% efficiency (using Dehmelt's 'electron shelving' technique [2, 18, 19]). We assume that the Ramsey separated field method is used in the time domain to interrogate the clock transition at frequency ω_0 (in rad s^{-1}). In this method, excitation of the clock transition is by

two phase-coherent pulses of radiation, each of duration ΔT_R, separated by a time T_R. We assume that $\Delta T_R \ll T_R$. By probing the clock transition on each side of the Ramsey peak, we can obtain an error signal to drive the average frequency to ω_0. The frequency stability for the locked oscillator as characterized by the two-sample Allan variance [20] is

$$\sigma_y(\tau) = (\tau N T_R \omega_0^2)^{-1/2}, \qquad (\tau > T_R), \tag{5}$$

where τ is the averaging time and N is the number of atoms. This expression shows that there is an advantage in using large N, ω_0, T_R, and τ. The trap environment can enable long interrogation times T_R. To achieve high accuracy, we must minimize and account for external perturbations due to electric, magnetic, and gravitational fields. These include ion–trap and ion–ion interactions, collisions with neutral background atoms, external magnetic and electric fields, and gravitational red shifts. For a microwave transition on a cold string of $^{199}Hg^+$ ions, the uncertainty could eventually be as small as the uncertainty of the second-order Doppler shift. At the Doppler limit of laser cooling, the fractional second order Doppler shift of $^{199}Hg^+$ is $-2{\cdot}3 \times 10^{-18}$ [4]. To realize this small Doppler shift it will be necessary that the equilibrium radial position of the ions coincide exactly with the line along which the r.f. trapping fields vanish. Otherwise, the micromotion will cause the second-order Doppler shifts to be much larger. The contributions of other effects, such as Stark shifts due to neighbouring ions, are discussed in [21, 22].

This potential for very high accuracy has led us to investigate the possibility of a microwave frequency standard based on the 40·5 GHz ground-state hyperfine splitting of $^{199}Hg^+$ with a trapped and laser-cooled string of ions. This transition is independent of the magnetic field to first order at zero field. For a Ramsey interrogation time of $T_R = 100$ s and $\omega_0/2\pi = 40{\cdot}5$ GHz, the frequency stability of a clock 'ensemble' of $N = 50$ ions would be $\sigma_y(\tau) = 5{\cdot}5 \times 10^{-14} \tau^{-1/2}$.

As a first step toward this goal we have recently detected the 40·5 GHz ground-state hyperfine transition of a string of $^{199}Hg^+$ ions by microwave–optical double-resonance. For this preliminary measurement the total fluorescence of the whole string of ions was measured. This meant that the measurement was sensitive to noise arising from intensity and frequency fluctuations in the cooling/detecting laser, so the stability figure given by equation (5) is not applicable.

To describe the measurement sequence we rely on the discussion of laser cooling and optical pumping given in the previous section and on figure 4. As described above, when the lasers are on, it is necessary to apply a magnetic field to prevent optical pumping into the ($F=1$, $m_F = \pm 1$) levels of the ground-state. However, to avoid second-order Zeeman shifts of the $(F=1)-(F=0)$ ground-state hyperfine interval, we wanted to have zero magnetic field during the measurement. To this end, we used two sets of Helmholtz coils. One set cancelled the ambient field and the second set applied a field of about 5×10^{-4} T (5 G) to prevent optical pumping. With the second set of coils switched off, the residual magnetic field near the trap was measured to be approximately $1{\cdot}6 \times 10^{-5}$ T (0·16 G). The sequence of the measurement is as follows:

(*a*) Lasers 1 and 2 and the magnetic field are all initially on to laser-cool the ions.
(*b*) Laser 2 is turned off and the ions are optically pumped by laser 1 into the $F=0$ ground-state.

(*c*) Both lasers are turned off, the second set of Helmholtz coils are switched off, bringing the magnetic field near zero. The $^2S_{1/2}(F=0)\rightarrow{}^2S_{1/2}(F=1)$ hyperfine transition near 40·5 GHz is driven using the Ramsey method with two microwave pulses, each of duration ΔT_R and separated by a time T_R. ΔT_R and the microwave power are adjusted to be close to values that give a $\pi/2$ pulse at the resonant frequency.

(*d*) The magnetic field is switched back to the value at step (*a*), laser 1 is turned on, and we measure flurorescence from the ions. The fluorescence is proportional to the number of ions (driven by the microwaves) that have made the transition to the $^2S_{1/2}(F=1)$ state.

At the end of this sequence, the frequency of the microwave source is stepped, and the sequence is repeated. The results of many such scans are averaged together. The results of such a measurement, made with eight ions and $T_R = 1{\cdot}8$ s, is shown in figure 7. The line centre and linewidth were determined from a least-squares fit of a cosine function to the central lobe of the observed Ramsey spectrum. For the signal-to-noise ratio of this spectrum, the difference between a cosine function and an exact Ramsey profile is insignificant. The measured linewidth is 251 ± 6 mHz, which gives

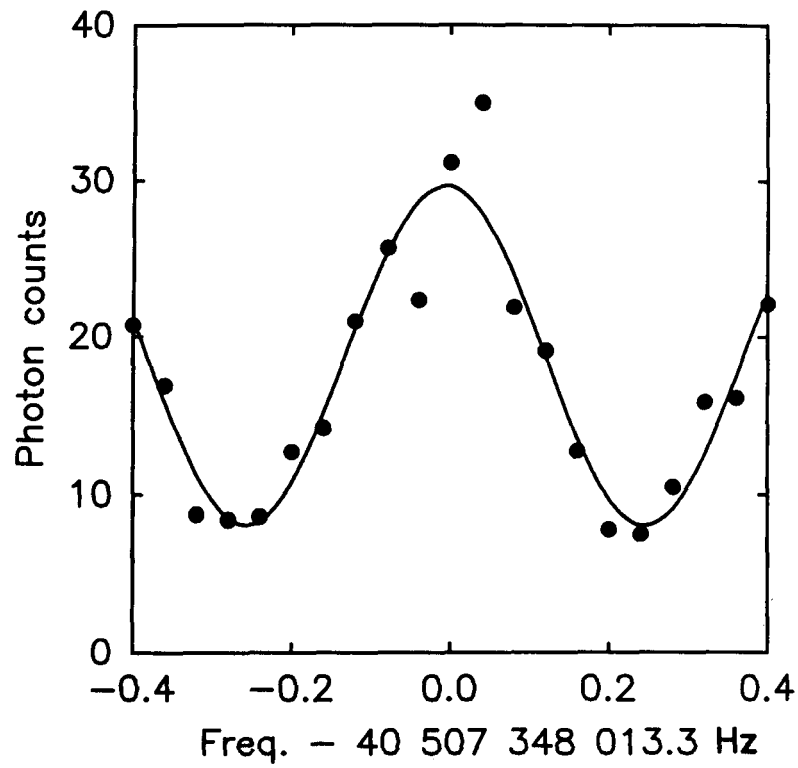

Figure 7. Microwave–optical double-resonance of the $^2S_{1/2}(F=0)\rightarrow{}^2S_{1/2}(F=1)$ hyperfine splitting of $^{199}Hg^+$ at 40·5 GHz. Shown is the central peak of a Ramsey resonance with the measurement sequence as described in the text, taken with a linear string of eight ions. The circles represent data; the solid line is a cosine function fit to the data using the least-squares criterion. For this measurement $T_R = 1{\cdot}8$ s, $\Delta T_R = 130$ ms, and each point is the average of 27 measurements. Including time for cooling, pumping and detection, each measurement cycle takes about 3 s.

a fractional resolution of $6{\cdot}2 \times 10^{-12}$. The theoretical linewidth for the pulse duration and free precession times used in this measurement is 254 mHz, in good agreement with the data.

For future experiments, in which the individual ions will be monitored separately, the fluorescence detection efficiency must be high enough that when laser 1 is turned on, enough photons will be detected that we can be sure whether each ion has or has not made the microwave transition. The number of photons scattered by an ion before it is pumped into the $^2S_{1/2}(F=0)$ level is approximately equal to the square of the ratio of 6·9 GHz (the detuning of laser 1 from the $^2S_{1/2}(F=1) \rightarrow {}^2P_{1/2}$ $(F=1)$ transition) to 35 MHz (half the radiative linewidth). This gives about 40 000 photons if laser 1 is resonant with the $^2S_{1/2}(F=1) \rightarrow {}^2P_{1/2}(F=0)$ transition. Therefore, the detection efficiency must be significantly better than the inverse of this number which is 3×10^{-5}. If this condition is met, it should be possible to detect the microwave transitions in each ion with nearly 100% efficiency. We have measured the detection efficiency of the present apparatus to be near 10^{-4}, which is marginally acceptable.

5. Future prospects

To reach the very high accuracy which should be possible with such a clock, it will be advantageous to use longer interrogation times. To reduce heating caused by collisions with background neutral atoms during the interrogation time, cryogenic pumping or sympathetic cooling [23] will most likely be required. Although in our preliminary measurements the total fluorescence from the entire string was measured, it appears possible to measure the fluorescence from each ion individually. It is then a data handling problem to route the counts from each ion to the correct 'bin' in the servo electronics.

Beyond the applications to high-accuracy spectroscopy, confining a string of ions so that each is in the Lamb–Dicke regime should make it possible to perform interesting experiments in fundamental physics such as studies of interference, cavity QED, collective behavior, and the fundamental quantum noise in the measurement of a transition in a single atom.

Acknowledgments

We gratefully acknowledge the support of the U.S. Office of Naval Research and and the Air Force Office of Scientific Research. We thank F. Moore and H. Robinson for helpful suggestions on the manuscript.

References

[1] Janik, G., Nagourney, W., and Dehmelt, H., 1985, *J. opt. Soc. Am.* B, **2,** 1251.
[2] Bergquist, J. C., Itano, W. M., and Wineland, D. J., 1987, *Phys. Rev.* A, **36,** 428.
[3] Itano, W. M., and Wineland, D. J., 1982, *Phys. Rev.* A, **25,** 35; Wineland, D. J., and Itano, W. M., 1987, *Phys. Today,* **40** (6), 34.
[4] Wineland, D. J., Itano, W. M., Bergquist, J. C., and Hulet, R. G., 1987, *Phys. Rev.* A, **36,** 2220; Wineland, D. J., Itano, W. M., Bergquist, J. C., Bollinger, J. J., Diedrich, F., and Gilbert, S. L., 1989, *Frequency Standards and Metrology,* Proceedings of the fourth Symposium, edited by A. DeMarchi (Berlin: Springer-Verlag), pp. 71–77.
[5] Wineland, D. J., 1984, *Precision Measurement and Fundamental Constants II,* edited by B. N. Taylor and W. D. Phillips (National Bureau of Standards (U.S.) Spec. Publ. 617), p. 83.
[6] DeVoe, R. G., Hoffnagle, J., and Brewer, R. G., 1989, *Phys. Rev.* A, **39,** 4362.

[7] BLÜMEL, R., KAPPLER, C., QUINT, W., and WALTHER, H., 1989, *Phys. Rev.* A, **40,** 808.
[8] DREES, J., and PAUL, W., 1964, *Z. Phys.*, **180,** 340.
[9] CHURCH, D. A., 1969, *J. appl. Phys.*, **40,** 3127.
[10] DEHMELT, H. G., 1989, *Frequency Standards and Metrology*, Proceedings of the fourth Symposium, edited by A. DeMarchi (Berlin: Springer-Verlag), p. 286.
[11] PRESTAGE, J. D., DICK, G. J., and MALEKI, L., 1989, *J. appl. Phys.*, **66,** 1013; PRESTAGE, J. D., DICK, G. J., and MALEKI, L., 1991, *I.E.E.E. Trans. Instrum. Meas.*, **40,** 132.
[12] WALTHER, H., 1991, *Light Induced Kinetic Effects on Atoms, Ions and Molecules*, Proceedings Workshop Elba Island, Italy May 2–5, 1990, edited by L. Moi *et al.* (Pisa: ETS Editrice), p. 261; BIRKL, G., KASSNER, S., QUINT, W., and WALTHER, H., Max Planck Institute for Quantum Optics, private communication.
[13] RAIZEN, M. G., BERGQUIST, J. C., ITANO, W. M., and WINELAND, D. J., 1991, *Conference on Quantum Electronics and Laser Science*, Talk QWE3, Baltimore, MD.
[14] PAUL, W., REINHARD, H. P., and VON ZAHN, U., 1958, *Z. Phys.*, **152,** 143.
[15] WINELAND, D. J., BERGQUIST, J. C., BOLLINGER, J. J., ITANO, W. M., HEIZEN, D. J., GILBERT, S. L., MANNEY, C. H., and RAIZEN, M. G., 1990, *I.E.E.E. Trans. Ultrasonics, Ferroelectrics, and Frequency Control*, **37,** 515; ITANO, W. M., BERGQUIST, J. C., and WINELAND, D. J., *Proceedings of Crystalline Ion Beams*, Wertheim, W. Germany, edited by R. W. Hasse, I. Hofmann and D. Liese (GSI report GSI-89-10, ISSN 0170-4546), p. 241.
[16] HASSE, R. W., and SCHIFFER, J. P., 1990, *Ann. Phys. N.Y.*, **203,** 419; HASSE, R. W., and SCHIFER, J. P., *Proceedings of Workshop on Crystalline Ion Beams*, Wertheim, W. Germany, edited by R. W. Hasse, I. Hofmann and D. Liese (GSI report GSI-89-10, ISSN 0170-4546), p. 33; HABS, D., *Ibid.*, p. 43.
[17] WINELAND, D. J., BOLLINGER, J. J., and ITANO, W. M., 1983, *Phys. Rev. Lett.*, **50,** 628.
[18] NAGOURNEY, W., SANDBERG, J., and DEHMELT, H., 1986, *Phys. Rev. Lett.*, **56,** 2797.
[19] SAUTER, TH., NEUHAUSER, W., BLATT, R., and TOSCHEK, P. E., 1986, *Phys. Rev. Lett.*, **57,** 1696; SAUTER, TH., BLATT, R., NEUHAUSER, W., and TOSCHEK, P. E., 1986, *Optics Commun.*, **60,** 287.
[20] BARNES, J. A., CHI, A. R., CUTLER, L. S., HEALEY, D. J., LEESON, D. B., MCGUNIGAL, T. E., MULLEN, J. A., JR., SMITH, W. L., SNYDOR, R. L., VESSOT, R. F. C., and WINKLER, G. M. R., 1971, *I.E.E.E. Trans. Instrum. Meas.*, **20,** 105.
[21] ITANO, W. M., LEWIS, L. L., and WINELAND, D. J., 1982, *Phys. Rev.* A, **25,** 1233.
[22] WINELAND, D. J., ITANO, W. M., BERGQUIST, J. C., BOLLINGER, J. J., and PRESTAGE, J. D., 1985, *Ann. Phys.* (Paris) **10,** 737.
[23] LARSON, D. J., BERGQUIST, J. C., BOLLINGER, J. J., ITANO, W. M., and WINELAND, D. J., 1986, *Phys. Rev. Lett.*, **57,** 70.